

1 *Supplementary of*

2 **Characterizing water solubility of fresh and aged secondary organic**
3 **aerosol in PM_{2.5} with the stable carbon isotope technique**

4

5 Fenghua Wei¹, Xing Peng¹, Liming Cao¹, Mengxue Tang¹, Ning Feng¹, Xiaofeng Huang¹, Lingyan
6 He¹

7 ¹Laboratory of Atmospheric Observation Supersite, School of Environment and Energy, Peking
8 University Shenzhen Graduate School, Shenzhen 518055, China.

9 **Correspondence:** Xing Peng (pengxing@pku.edu.cn)

10 **Contents of this file**

11 **Text S1 - Text S2**

12 Text S1. PMF model and results

13 Text S2. Sampling of potential emission sources of carbonaceous aerosol

14 **Figure S1 - Figure S5**

15 Figure S1. Seasonal backward trajectory of air masses in Shenzhen, 2019. (a) spring (b) summer (c) fall
16 (d) winter.

17 Figure S2. The source profiles resolved by PMF for PM_{2.5}.

18 Figure S3. Source apportionment results of PM_{2.5} (a) and carbonaceous aerosol (b) based on the PMF
19 model. (c) The relative contribution of different sources to PM_{2.5} and carbonaceous fractions.

20 Figure S4. The source profiles resolved by PMF for WSOC.

21 Figure S5. Cumulative frequency distributions of the proportional contributions from potential sources
22 of TC (a) and WSOC (b) based on BSIM model.

23 **Table S1 - Table S3**

24 Table S1. Description of the sampling sites in Shenzhen.

25 Table S2. General meteorological conditions during the sampling period in 2019.

26 Table S3. Comparison of $\delta^{13}\text{C}_{\text{TC}}$ source signatures in this study with global datasets

27 **Text S1: PMF model and results**

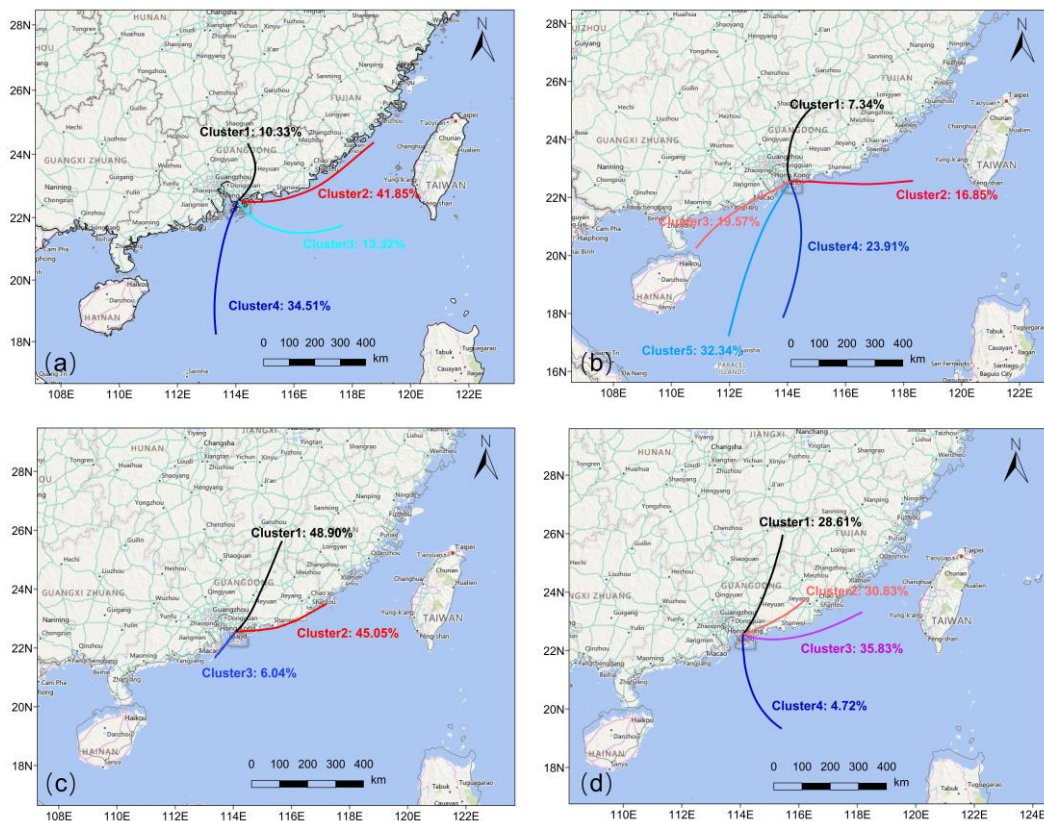
28 In this study, the PMF model (EPA PMF v5.0,) was employed to identify the sources of TC and WSOM.
29 The detailed fundamental principle of this model can be found in Paatero et al.(1994) (Paatero and Tapper
30 1994). The mass concentration and uncertainty values of seventeen indicative chemical components (OM,
31 EC, NH_4^+ , Cl^- , NO_3^- , SO_4^{2-} , Na, Mg, Al, K, Ca, V, Ni, Cd, Fe, Zn, and Pb) were put into this model to
32 calculate the contributions of different sources to TC. The information on the measurement of the
33 carbonaceous fractions is described in the main text. In addition, an Ion Chromatography Analyser (ICS-
34 2500, Dionex; Sunnyvale, California, USA) and Inductively Coupled Plasma Mass Spectrometry (ICP-
35 MS, Aurora M90; Bruker, Germany) were used for the mass concentration analysis of water-soluble ions
36 and metal elements respectively. Ten factors (vehicle emissions, ship emissions, aged sea salt,
37 construction dust, fugitive dust, coal combustion, industrial emissions, biomass burning, secondary
38 sulfate, and secondary nitrate) were identified, as shown in Fig. S2. SOA was then estimated from the
39 OM fraction in both secondary sulfate and secondary nitrate factors. To compare with BSIM results, the
40 source apportionment of TC was merged into three sources, including SOA, traffic emission, and biomass
41 burning (Fig. S3) (Zong et al., 2018). The industrial emission source and coal combustion source were
42 not included because of their little contribution to carbonaceous fraction. The remaining eight sources
43 were then reapportioned and then combined according to the contribution to OC and EC. Specifically,
44 the contributions of vehicle and ship emissions to EC and OC were attributed to the traffic source. The
45 contributions of secondary sulfate, secondary nitrate, and aged sea salt sources to OC were all attributed
46 to the SOA. The contributions of biomass burning source to OC were attributed to the BB (biomass
47 burning) source. The mass concentration and uncertainty values of five species (CO_2^+ , C_4H_9^+ , $\text{C}_2\text{H}_4\text{O}_2^+$,
48 WSOC, and WSOO) were put into the PMF model to calculate the contribution of three sources (BBOA

49 (biomass burning organic aerosol), LO-OOA (less-oxidized oxygenated OA), MO-OOA (more-oxidized
50 oxygenated OA)) to WSOM (Fig. S4).

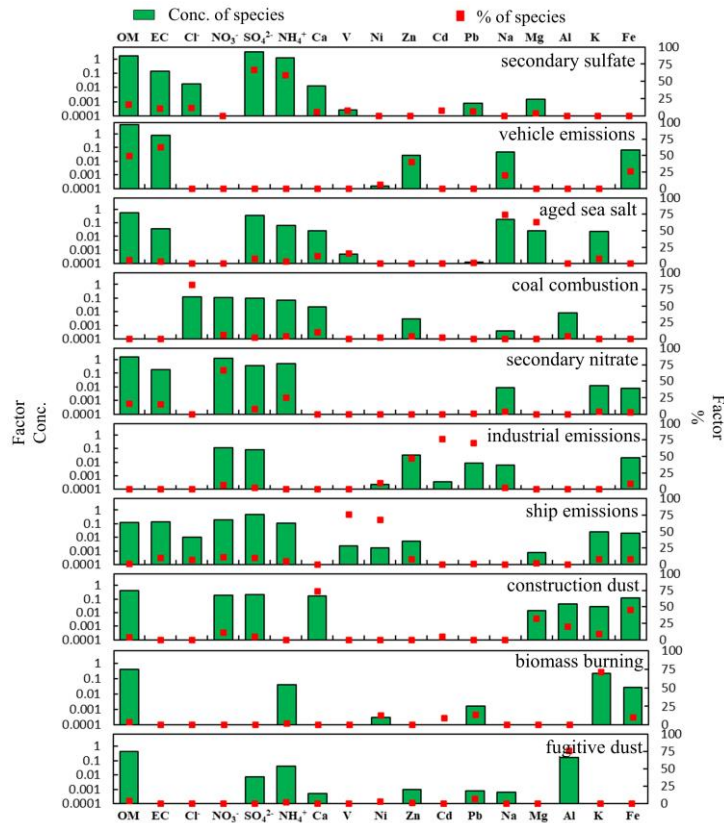
51 **Text S2: Sampling of potential emission sources of carbonaceous aerosol**

52 PM_{2.5} samples of four sources were collected from ambient air and simulation experiments to measure
53 the $\delta^{13}\text{C}$ values of TC and WSOC in this study. We collected PM_{2.5} samples from two tunnel sites (Mount
54 Tanglang tunnel and Jiuweiling tunnel), which can comprehensively reflect the vehicle emissions level
55 to ambient air in Shenzhen because of its specificity of the environment. Two medium-flow samplers
56 (KC-120H model, Qingdao Laoshan, 100 L/min) were used in this sampling process. The lengths of
57 those two tunnels were 1711 m and 1447 m, representing the emission characteristics of diesel and petrol
58 vehicles in Shenzhen respectively. General information about the number of samples and sampling time
59 at each tunnel are provided in Table S4 and S5. Specifically, six samples were obtained from 23:00 to
60 02:10 and 02:30 to 05:30 on 13-18 October 2014 at the Mount Tanglang tunnel site. Additional eight
61 samples were subsequently collected at different periods (peak and off-peak traffic periods in both
62 daytime and night) on 20-22 January 2015 at the junction of one side of Mount Tanglang tunnel, and the
63 sampling durations ranged from 2.5 to 11.5 hours. A total of 11 samples were obtained at the Jiuweiling
64 tunnel site. The peak and off-peak traffic periods in both daytime and night were also included in this
65 sampling period, and the sampling durations ranged from 2 to 6 hours. For fresh SOA, five PM_{2.5}
66 samples from petrol vehicle bench tests conducted under different fuel types and operating conditions
67 were collected. Detailed information about this test system was displayed in Zheng et al. (2017) (Zheng
68 2017). Two parallel samples were collected and measured under each operating condition to ensure the
69 reliability of the measured data. Two aged SOA samples were collected at the national ambient air
70 background monitoring station in Mount Wuzhi, Hainan Province, from 13-15 April 2015. A complete

71 secondary transport process was captured during this sampling period, and each sampling duration was
 72 23.5 hours. Lastly, We collected three PM_{2.5} samples representing the biomass combustion source
 73 through biomass combustion simulation experiment (He et al., 2010), of which were conducted in the
 74 combustion simulation laboratory at Peking University Shenzhen Graduate School on 24-28 May 2017.
 75 Pine branches, as a major source of biomass burning in south China (Chen et al., 2017) were selected as
 76 the representative plant for the combustion simulation experiment in this study. The pine branches were
 77 divided into three weight groups (low (3 kg), medium (6 kg) and high (8 kg)). Samples at three different
 78 combustion stages (ignition, flame combustion, and complete combustion) were collected, and the
 79 sampling time at each stage was 49, 75, and 90 minutes, respectively. Each sampling and analysis process
 80 was repeated three times to ensure reliability.



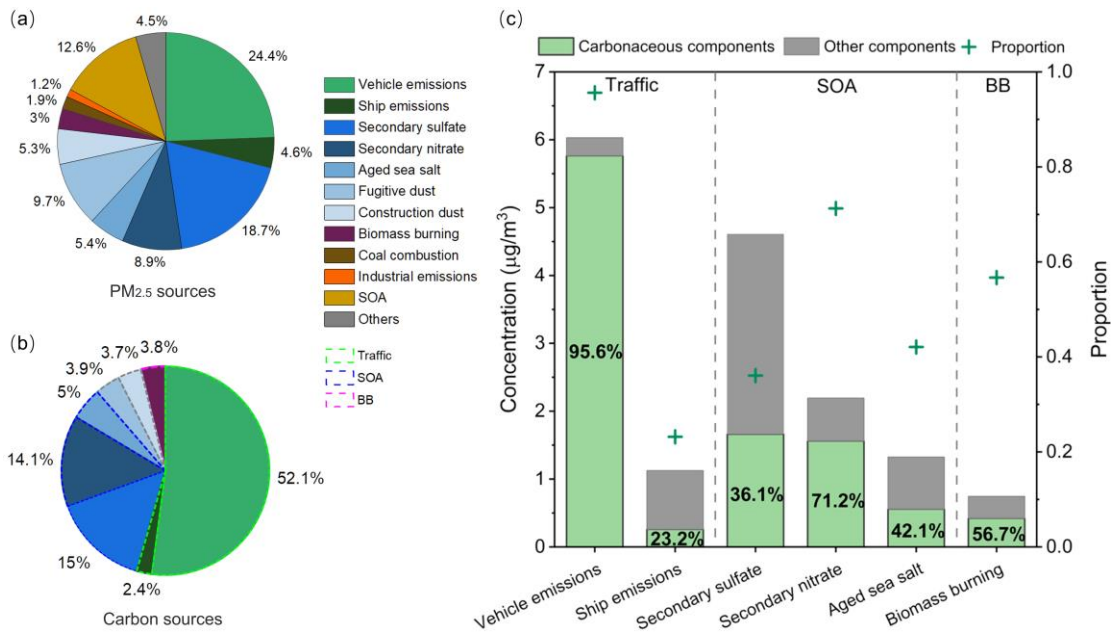
81
 82 **Figure S1.** Seasonal backward trajectory of air masses in Shenzhen, 2019. (a) spring (b) summer (c) fall
 83 (d) winter. Map image: © Microsoft by MeteoInfoMap.



84

85

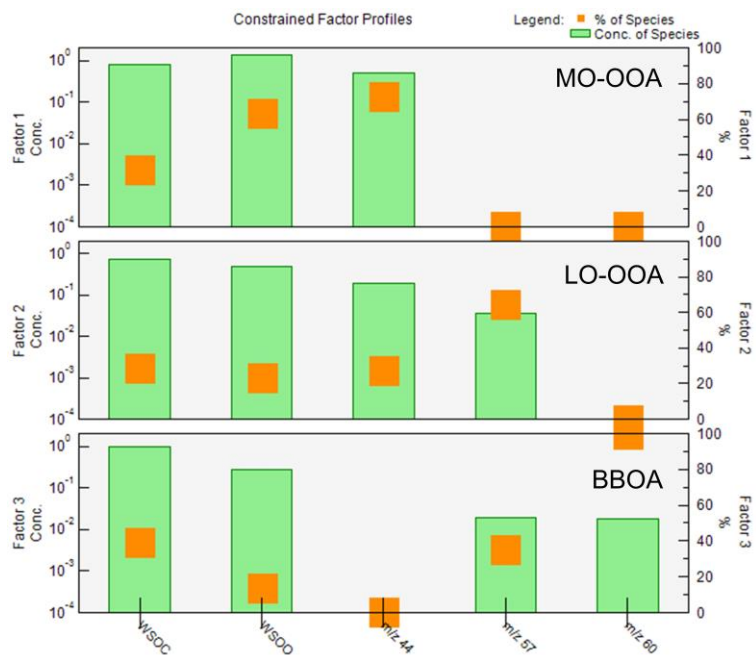
Figure S2. The source profiles resolved by PMF for PM_{2.5}.



86

Figure S3. Source apportionment results of PM_{2.5} (a) and carbonaceous aerosol (b) based on the PMF

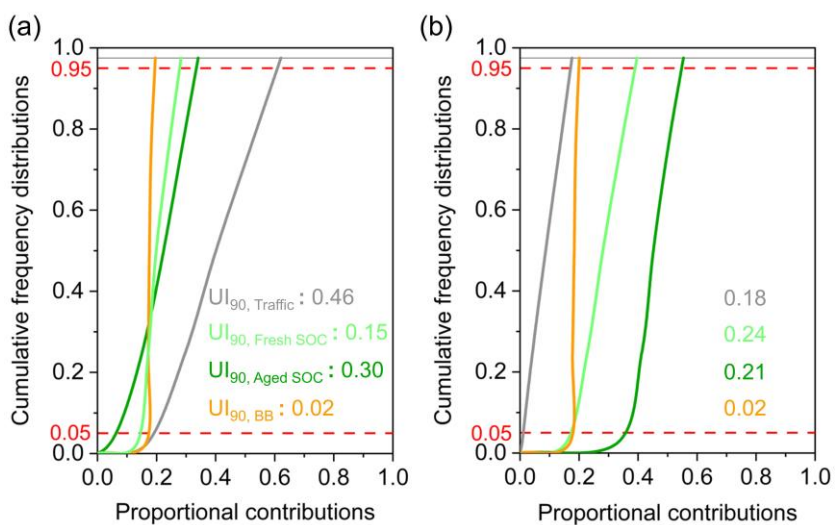
88 model. (c) The relative contribution of different sources to PM_{2.5} and carbonaceous fractions.



89

90

Figure S4. The source profiles resolved by PMF for WSOC.



91

92 **Figure S5.** Cumulative frequency distributions of the proportional contributions from potential sources

93 of TC (a) and WSOC (b) based on BSIM model.

94 **Table S1.** Description of the sampling sites in Shenzhen.

Site	Site Code	Coordinates	Site description
University town	UT	Lat: 22.59°N Long: 113.97°E	Urban This site reflects the pollution characteristics of typical urban areas and regional transport
Longhua	LH	Lat: 22.68°N Long: 114.01°E	Urban This site generally reflects the pollution characteristics of urban local emissions
Honghu	HH	Lat: 22.57°N Long: 114.14°E	Urban This site reflects the pollution characteristics of the general urban areas
Xixiang	XX	Lat: 22.58°N Long: 113.90°E	Urban This site reflects the pollution characteristics of western industrial urban areas in Shenzhen
Dapeng	DP	Lat: 22.64°N Long: 114.42°E	Background This site reflects the pollution characteristics of the eastern coastal tourist areas

95

96 **Table S2.** General meteorological conditions during the sampling period in 2019.

	Mean temp. (°C)	Rainfall (mm)	Mean RH (%)	Mean wind speed (m s ⁻¹)	Predominant wind direction
Spring (1 Mar-8 Apr)	21.3	151.8	83.0	1.7	ESE
Summer (1 Jun-3 Jul)	28.5	275.8	85.0	2.2	SW
Autumn (1 Sept-11 Oct)	27.6	175.0	74.0	1.6	ESE
Winter (22 Nov-30 Dec)	19.5	3.2	62.0	2.0	NNE

97

98 **Table S3.** Comparison of $\delta^{13}\text{C}_{\text{TC}}$ source signatures in this study with global datasets.

Emission sources	Continent	Location	Sample types	$\delta^{13}\text{C}(\text{‰})$	SD	Ref.
	Asia(This study)	China, Shenzhen	Traffic	-26.26	0.50	-
	Asia	China	Wucun Tunnel, Entrance	-25.84	0.23	
	Asia	China	Wucun Tunnel, Exit	-25.88	0.24	(Yao et al., 2022)
	Asia	China	Xianyueshan Tunnel, Entrance	-25.88	0.26	
	Asia	China	Xianyueshan Tunnel, Exit	-25.79	0.23	
	Asia	Guangzhou	Traffic	-24.6 to -25.5		(Dai et al., 2015)
	Asia	India	Traffic	-25.3	0.3	(Agnihotri et al., 2011)
	Asia	Nepal	Traffic	-26.5 to -26.1		(Shakya;Ziemba and Griffin 2010)
	Asia	China	Traffic	-25.85	0.22	(Yao et al., 2022)
	Asia	China	Traffic	-25.27	0.32	(Chen et al., 2012)
Traffic	Asia	Pearl River Delta	Gasoline exhaust	-28.6	0.6	
	Asia	Pearl River Delta	Diesel exhaust	-27.8	0.2	
	Asia	China	Zhujiang Tunnel, Vehicle emissions	-25	0.3	(Dai et al.,2013)
	Asia	India	Diesel exhaust	-26.3	0.2	
	Asia	India	Bio-diesel exhaust	-26.5	0.1	(Singh et al., 2018)
	Asia	India	Petrol(Gasoline) exhaust	-26.1	0.01	
	North America	Mexico	Tunnel; Diesel vehicle emissions	-24.6	0.3	
	North America	Mexico	Tunnel; Gasoline vehicle emissions	-25.5	0.1	(López-Veneroni 2009)
	Oceania	New Zealand	Mount Victoria Tunnel	-25.9	0.8	(Ancelet et al., 2011)
	Europe	Germany	Gasoline exhaust	-26.2	0.2	(Fisseha et al., 2009)
	Europe	Paris	Diesel exhaust	-26.5	0.5	(Widory et al., 2004)
	Europe	Germany	Diesel exhaust	-27.6	0.01	(Fisseha et al., 2009)
	Europe	Paris	Complete combustion of diesel	-29		(Widory 2006)

	Europe	Paris	Complete combustion of gasoline	-27		(Widory 2006)
	Europe	Paris	Fuel oil exhaust	-26.5	0.5	(Widory et al., 2004)
	Europe	Krakow, Poland	Traffic	-30	1	(Zimnoch et al., 2020)
	worldwide	worldwide	Traffic group1	-26.8	1.1	
	worldwide	worldwide	Traffic group2	-28.9	1.7	(Yao et al., 2022)
	worldwide	worldwide	Traffic group3	30.2	0.9	
	Asia(Our study)	China, Hainan	Aged SOC , ambient samples of the Mount Wuzhi	-25.54	0.28	-
	Asia(Our study)	China, Shenzhen	Fresh SOC , petrol vehicle bench tests	-27.31	0.73	
SOA	Europe	Germany	Compounds in SOA: aerosol-phase nopinone	-27.6 to -24.8		
	Europe	Germany	Compounds in SOA: acetone	-35.1 to -38.6		
	Europe	Germany	Compounds in SOA: gas-phase nopinone	-28.8		(Fisseha et al., 2009)
	Europe	Germany	Precursor of SOA: initial β -pinene injected	-30.1		
	Europe	Germany	Precursors of SOA	-29.6	0.2	
	North America	Canada	Secondary particulate organic matter			(Irei et al., 2011)
	North America	Canada,	Secondary particulate organic matter	-32.2 to -32.9		(Irei et al., 2006)
	Asia(Our study)	China, Shenzhen	Burning experiment results of pine branches	-27.58	0.24	-
	worldwide	worldwide	C3 plant	-27.2	1.6	
	Asia	China	C3 plant	-27.89	0.26	(Yao et al., 2022)
	Asia	China	Seven C3 plants	-27.12		
	Asia	China	Biomass burning (Seven C3 plants)	-26.99	1.11	
BB	America	Texas	C3 plant	-27	6	(Boutton 1991)
	Europe	Krakow, Poland	Biomass burning(C3 plants)	-26	2	(Zimnoch et al., 2020)
	Asia	China	C4 smoldering	-14.25		
	Asia	China	C4 flaming	-18.42		
	Asia	China	C4 plant (corn stalk)	-12		(Yao et al., 2022)
	Asia	China	Biomass burning (corn stalk)	-13.09		
	worldwide	worldwide	C4 plant	-13.2	1.1	
	America	Texas	C4 plant	-13	4	(Boutton 1991)

100 **References**

- 101 Agnihotri, R., Mandal, T. K., Karapurkar, S. G., Naja, M., Gadi, R., Ahammed, Y. N., Kumar, A., Saud,
102 T. & Saxena, M. (2011) Stable carbon and nitrogen isotopic composition of bulk aerosols over India
103 and northern Indian Ocean. *Atmos. Environ.*, 45, 2828-2835.
- 104 Ancelet, T., Davy, P. K., Trompetter, W. J., Markwitz, A. & Weatherburn, D. C. (2011) Carbonaceous
105 aerosols in an urban tunnel. *Atmos. Environ.*, 45, 4463-4469.
- 106 Boutton, T. W. 1991. 11 – Stable carbon isotope ratios of natural materials: II. atmospheric, terrestrial,
107 marine, and freshwater environments.
- 108 Chen, Y., Wenger, J. C., Yang, F. M., Cao, J. J., Huang, R. J., Shi, G. M., Zhang, S. M., Tian, M. & Wang,
109 H. B. (2017) Source characterization of urban particles from meat smoking activities in Chongqing,
110 China using single particle aerosol mass spectrometry. *Environ. Pollut.*, 228, 92-101.
- 111 Chen, Y. J., Cai, W. W., Huang, G. P., Li, J. & Zhang, G. (2012) Stable carbon isotope of black carbon
112 from typical emission sources in China. *Environ. Sci.*, 33, 673-8.
- 113 Dai, S., Bi, X., Chan, L. Y., He, J., Wang, B., Wang, X., Peng, P., Sheng, G. & Fu, J. (2015) Chemical
114 and stable carbon isotopic composition of PM_{2.5} from on-road vehicle emissions in the PRD region
115 and implications for vehicle emission control policy. *Atmos. Chem. Phys.*, 15, 3097-3108.
- 116 Fisseha, R., Spahn, H., Wegener, R., Hohaus, T., Brasse, G., Wissel, H., Tillmann, R., Wahner, A.,
117 Koppmann, R. & Kiendler-Scharr, A. (2009) Stable carbon isotope composition of secondary organic
118 aerosol from β -pinene oxidation. *J. Geophys. Res. Atmos.*, 114.
- 119 He, L. Y., Lin, Y., Huang, X. F., Guo, S., Xue, L., Su, Q., Hu, M., Luan, S. J. & Zhang, Y. H. (2010)
120 Characterization of high-resolution aerosol mass spectra of primary organic aerosol emissions from
121 Chinese cooking and biomass burning. *Atmos. Chem. Phys.*, 10, 11535-11543.
- 122 Irei, S., Huang, L., Collin, F., Zhang, W., Hastie, D. & Rudolph, J. (2006) Flow reactor studies of the
123 stable carbon isotope composition of secondary particulate organic matter generated by OH-radical-
124 induced reactions of toluene. *Atmos. Environ.*, 40, 5858-5867.
- 125 Irei, S., Rudolph, J., Huang, L., Auld, J. & Hastie, D. (2011) Stable carbon isotope ratio of secondary
126 particulate organic matter formed by photooxidation of toluene in indoor smog chamber. *Atmos.*
127 *Environ.*, 45, 856-862.
- 128 López-Veneroni, D. (2009) The stable carbon isotope composition of PM_{2.5} and PM₁₀ in Mexico City

129 Metropolitan Area air. *Atmos. Environ.*, 43, 4491-4502.

130 Paatero, P. & Tapper, U. (1994) Positive matrix factorization: a nonnegative factor model with optimal
131 utilization of error estimates of data values. *Environmetrics.*, 5, 111-126.

132 Shakya, K. M., Ziemba, L. D. & Griffin, R. J. (2010) Characteristics and Sources of Carbonaceous, Ionic,
133 and Isotopic Species of Wintertime Atmospheric Aerosols in Kathmandu Valley, Nepal. *Aerosol Air*
134 *Qual Res.*, 10, 219-U13.

135 Singh, G. K., Rajput, P., Paul, D. & Gupt, T. (2018) Wintertime study on bulk composition and stable
136 carbon isotope analysis of ambient aerosols from North India. *J Aerosol Sci.*, 126, 231-241.

137 Widory, D. (2006) Combustibles, fuels and their combustion products: A view through carbon isotopes.
138 *Combust. Theory Model.*, 10, 831-841.

139 Widory, D., Roy, S., Le Moullec, Y., Goupil, G., Cocherie, A. & Guerrot, C. (2004) The origin of
140 atmospheric particles in Paris: a view through carbon and lead isotopes. *Atmos. Environ.*, 38, 953-
141 961.

142 Yao, P., Huang, R. J., Ni, H. Y., Kairys, N., Yang, L., Meijer, H. A. J. & Dusek, U. (2022) ¹³C signatures
143 of aerosol organic and elemental carbon from major combustion sources in China compared to
144 worldwide estimates. *Sci. Total Environ.*, 810.

145 Zheng, J. 2017. Source apportionment of organic aerosols and contribution of secondary formation from
146 vehicle emissions. Peking university.

147 Zimnoch, M., Samek, L., Furman, L., Styszko, K., Skiba, A., Gorczyca, Z., Galkowski, M., Rozanski, K.
148 & Konduracka, E. (2020) Application of natural carbon isotopes for emission source apportionment
149 of carbonaceous particulate matter in urban atmosphere: a case study from Krakow, southern Poland.
150 *Sustainability.*, 12.

151 Zong, Z., Tan, Y., Wang, X., Tian, C., Fang, Y., Chen, Y., Fang, Y., Han, G., Li, J. & Zhang, G. (2018)
152 Assessment and quantification of NO_x sources at a regional background site in North China:
153 Comparative results from a Bayesian isotopic mixing model and a positive matrix factorization model.
154 *Environ. Pollut.*, 242, 1379-1386.

155